my-614
galley proof

New Diamond and Frontier Carbon Technology
Vol. 16, No. 6 2006
MYU Tokyo

NDFCT 000

Synthesis of Ultrananocrystalline Diamond Films by Microwave Plasma-Assisted Chemical Vapor Deposition

Dzung T. Tran, Wen-Shin Huang, Jes Asmussen*, Timothy A. Grotjohn and Donnie K. Reinhard

Michigan State University, 2120 Engineering Building,
Electrical & Computer Engineering Department, East Lansing, MI 48824, USA
Fraunhofer USA, Center for Coatings and Laser Applications, B100 Engineering Research Complex, Michigan State University, East Lansing, Michigan 48826-1226, USA

(Received 9 March 2006; accepted 6 April 2006)

Key words: ultrananocrystalline diamond, diamond synthesis, microwave plasma processing

In this paper, we report on the development of process methods and apparatus that enable the deposition of ultrananocrystalline diamond (UNCD) films over a wide pressure range (60–180 Torr) and temperature range (400–800°C). The films are deposited using a microwave plasma-assisted chemical vapor deposition (MPCVD) system operating at 2.45 GHz with variable power and pressure. The influence of various input parameters such as feed gas mixture, pressure, and substrate temperature on the growth rate and surface morphology/roughness of the UNCD diamond films is investigated. Feed gas mixtures studied include argon-methane-hydrogen, helium-methane-hydrogen and argon-methane-nitrogen. Experimental data is reported for the growth rate, crystal size distribution, surface roughness, Young's modulus, and electrical conductivity.

1. Introduction

Ultrananocrystalline diamond (UNCD) is a diamond film/material that is synthesized by microwave plasma-assisted chemical vapor deposition (MPCVD) from hydrogen-poor argon/hydrogen/methane gas mixtures.(1) The name ultrananocrystalline is derived from the fact that these synthesized diamond films have grain sizes that range from a few to ten nanometers. UNCD films have exceptional properties that make them attractive for a variety

*Corresponding author: e-mail: asmussen@egr.msu.edu

of commercial applications. As a result of their small grain size, UNCD films can be deposited with very smooth surfaces. Thus, UNCD films are readily available for specific applications without the need for extensive postprocessing steps such as lapping. The UNCD films' mechanical and tribological properties, such as hardness, Young's modulus, and low friction, approach those of diamond.[2,3] Their electronic properties such as electrical conductivity of UNCD films can be varied by adding nitrogen during the deposition process[4] and they are inert to chemical attack.[5] This constellation of properties suggest that UNCD films are promising materials for many applications such as a low-friction, protective, hard, wear-resistance coating material, a material/substrate for micromechanical systems (MEMS),[6] a SAW device substrate,[7] a robust conducting coating for electrochemical electrodes,[5] and a biocompatible and biologically active substrate.[8]

As a UNCD material is evaluated in specific commercial applications, it is also necessary to investigate and develop UNCD process methods and equipment that are robust, repeatable and also have commercial potential. The commercial application of UNCD films imposes specific constraints on the synthesis process such as repeatability, uniform deposition over large areas, low-temperature deposition, and the deposition of thick (> 20 microns) and conducting films. These conditions require the development of process methodologies and associated deposition technologies that are robust, repeatable and meet the required application specific film criteria, such as uniform deposition over large areas, mechanical and electrical properties, and stress-free thin and thick films among others.

In this study MPCVD is investigated as the method to synthesize UNCD films. Both process methodologies and reactor process technologies are developed to enable the reliable and controllable deposition of large-area UNCD films. Described below are the results from a systematic experimental study wherein the potential of applying the MPACVD method and associated reactor technologies to synthesize commercially useful UNCD films is investigated. In this investigation, a specific microwave plasma reactor technology and a wide experimental UNCD deposition regime that are available for UNCD synthesis are identified. The deposition process relationships between the experimental input parameters and the output film properties are identified. The typical deposition process for UNCD synthesis[1] employs an argon rich feed gas mixed with low concentrations of methane and hydrogen. In this study, the potential of replacing the argon feed gas with helium is also investigated. The various potential applications of UNCD involve film properties that impose process constraints that often involve the trade-off of one process variable versus another. Thus, this investigation identifies an experimental methodology that is applied to process development and identifies a wide experimental UNCD deposition window that is available for process optimization.

2. Experimental Reactor System

A cross-sectional view of the microwave plasma reactor and the vacuum system is shown in Fig. 1. The experimental system consists of a variable power, 6 kW maximum, and 2.45 GHz microwave power supply that is connected to a 17.8-cm-diameter cylindrical microwave plasma cavity applicator.[9] As shown in the figure, the cavity applicator has a variable short and a variable-depth coupling probe; i.e., the cavity applicator is tunable. Microwave energy is coupled into the cavity applicator through the mechanically tunable coaxial

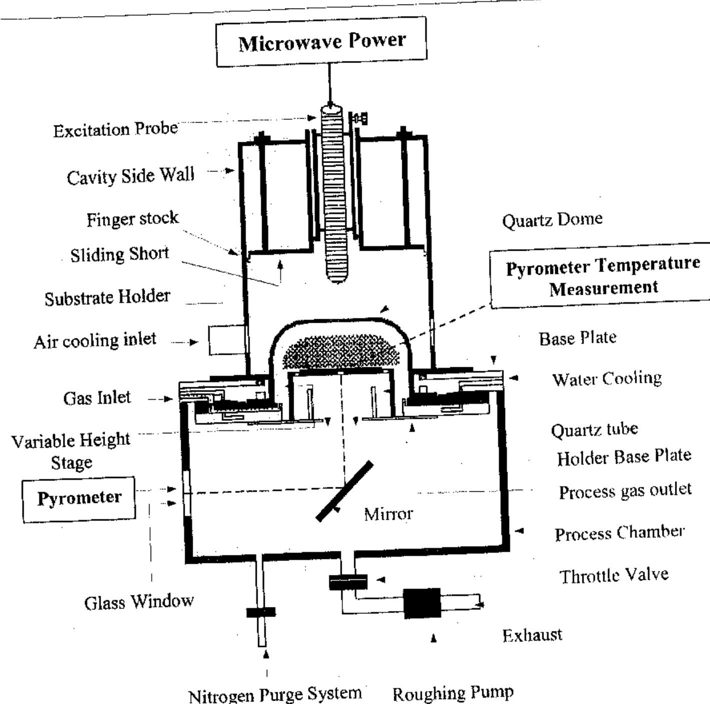

Fig. 1. Microwave cavity plasma reactor.

excitation probe. When the cavity applicator sliding short is adjusted to approximately 21.6 cm, the cavity applicator excites the TM_{013} mode and a hemispherical discharge is created and confined inside the 12.5 cm inside diameter cylindrical quartz dome which is located in the fixed base plate at the bottom of the applicator. A molybdenum substrate holder is placed on a stage located on the holder base plate. Process gases are introduced upward into the discharge region via a gas distribution ring located at the bottom flange of the quartz dome. The gases then flow through the discharge and out of the reactor via an annular ring of holes located on the outer rim of the substrate holder. Our experiments demonstrated that in order to routinely synthesize high-quality, smooth and uniform UNCD films, the deposition must be preformed in a high-purity environment.[10] Thus, experiments were carried out using a leak free vacuum system and with (1) argon, (2) H_2, (3) CH_4 source gas purities of 99.999%, and with (4) N_2, and (5) He source gas purities of 99.995%.

As shown in Fig.1, the silicon substrate was placed on the molybdenum holder. At each experimental operating pressure, the stage height and the cavity sliding short tuning were adjusted to position the substrate in direct contact with the microwave discharge. The discharge then assumes an intense, hemispherical shape hovering over and in direct contact with the substrate. The backside substrate temperature was measured by an optical pyrometer that viewed the backside of the substrate through several small, 3-mm-diameter holes that were located radially across and through the substrate holder. As is also shown in Fig. 1, the reactor base plate was water-cooled and the quartz dome was air cooled. Since

deposition repeatability was desired, the air and water-cooling temperatures were monitored and controlled so that process repeatability could be achieved. Additionally, the reactor was operated in a warm/hot condition to efficiently produce a thermally uniform deposition environment inside the quartz chamber.

All experiments were preformed using, as described elsewhere,[11,12] a thermally floating substrate configuration. In this configuration, the substrate holder and the substrate are not actively cooled or heated and thus all the energy supplied to the substrate is supplied by the microware discharge. The balance of heat flow from the discharge and the loss of heat due to conduction, radiation and convection determine the steady-state substrate temperature. When operating in this configuration, the substrate temperature is a function of both the pressure and the absorbed microwave power. That is, given a constant input chemistry, the major independent experimental variables, i.e., absorbed microwave power, P_{abs}, and pressure, p, have an experimentally repeatable, single-valued nonlinear relationship to the experimentally measured substrate temperature. Given a specific reactor configuration, gas input chemistry and flow rate, this nonlinear relationship can be measured. The resulting measured set of curves represents important curves that describe the experimentally useful operating UNCD deposition regions of the reactor system. Such a set of curves is identified here as the operating field map of the reactor.

Figures 2 and 3 show the operating field map for the reactor system shown in Fig. 1 when operating with the specific (100/4/1 sccm) $Ar/H_2/CH_4$ and $He/H_2/CH_4$ input gas chemistries. A similar set of operating curves can be produced for $Ar/CH_4/N_2$ input gas mixtures. As shown in the figures, the operation of the reactor at a given specific absorbed input power

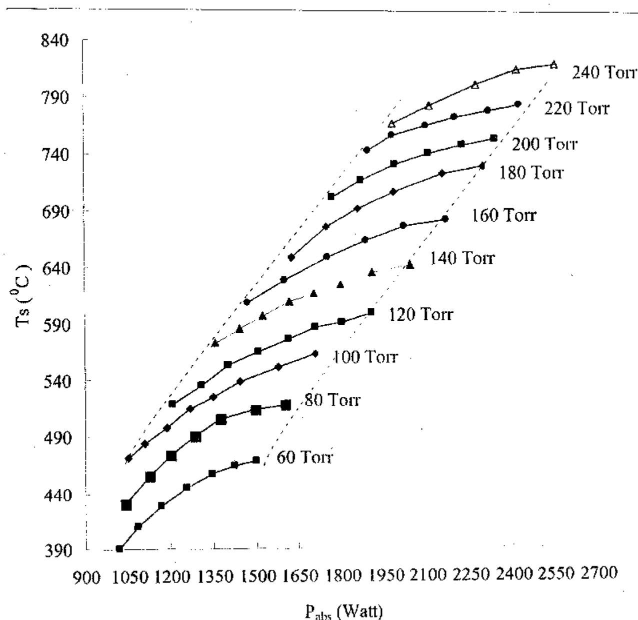

Fig. 2. MPACVD operating field map for $Ar\text{-}H_2\text{-}CH_4$ = 100-4-1 sccm.

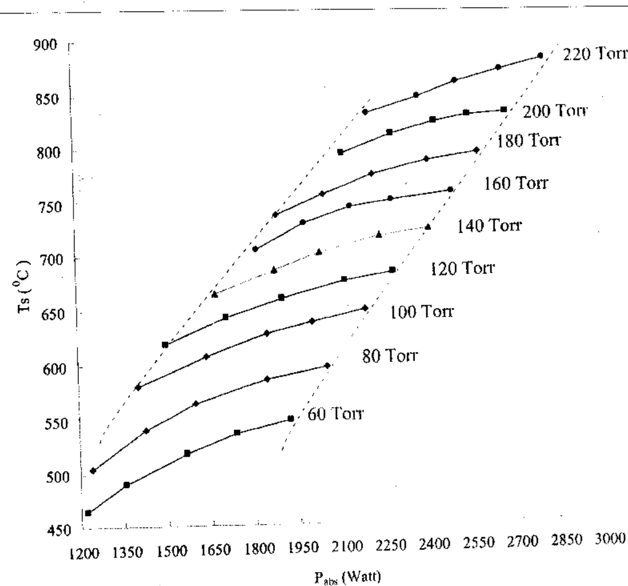

Fig. 3. MPACVD operating field map for $He\text{-}H_2\text{-}CH_4$ = 100-4-1 sccm.

and operating pressure results in a unique and repeatable substrate temperature. When the pressure constant is maintained and then the input power is independently increased or decreased, the discharge size is also correspondingly increased and decreased and the substrate temperature then traces out the curves as shown in Figs. 2 and 3. The left and right dashed lines in each figure represent for each pressure the allowable operating input power levels that yield useful UNCD deposition over a three inch silicon substrate. The left dashed line represents the minimum power required to form a 3-inch-diameter hemispherical discharge over the three inch wafer. Input power levels of less than this line limit will not produce uniform UNCD deposition over three inches. The right dashed line represents the input power at which the plasma expands to touch the quartz dome walls. Greater input powers cause dome heating and possibly undesirable plasma dome wall interactions. Thus, the field map curves in Figs. 2 and 3 define the reactor operating regimes within which to achieve optimum, uniform UNCD synthesis. Within this operating regime, the discharge is large enough in diameter to cover the 7.5-cm-diameter substrate and is small enough to not touch the walls of the 12.5-cm-diameter quartz dome.

Note that if input gas chemistry varies, i.e., the hydrogen concentration is changed from 0–4%, then the field map curves shift slightly. In particular, if the hydrogen concentration increases from 1 to 2%, the substrate temperature increases in the range of 10–25°C and as it increases from 2–4%, the substrate temperature increases by another 10–25°C. In a similar manner, the addition of molecular nitrogen also increases the substrate temperature. Thus, as the hydrogen chemistry is varied, another dimension related to the % amount to the input hydrogen gas can be added to the field map figures producing a three- dimensional field map and defining a three-dimensional volume in which UNCD synthesis can be achieved. The

experimental optimization of the process for a given application will take place within this field map volume.

3. Experimental Method

Similar to most plasma-assisted CVD processes, the synthesis of UNCD is a complex function of many experimental variables. The three basic variables groups[11] are (1) input variables, (2) internal variables, and (3) output variables. The input variables are the variables that can be independently controlled by an experimental operator or a reactor designer. The internal variables are the internal reactor states that can be measured such as substrate and gas temperature whereas the output variables are concerned with the reactor performance such as film growth rate and film quality.

Figure 4 shows the definition of the important input, internal and output experimental variables for this investigation. The critical output variables of this investigation are deposition rate, Young's modulus, smoothness, electrical conductivity, and uniformity. The important input variables are input pressure, absorbed microwave power and input feed gas mixture (type of inert gas, % hydrogen, % nitrogen and % methane). The critical internal variable is substrate temperature. Since the substrate is thermally floating, substrate temperature is not an independent experimental variable in this investigation.

A wide range of experimental conditions, i.e., pressure, input power, and flow rate were explored to identify the optimal conditions that enable the repeatable deposition of a uniform and smooth UNCD film over 3-inch-diameter silicon wafer substrates. The pressure range was varied from 60–180 Torr and the feed gases investigated included mixtures of argon-hydrogen-methane (99–95%, 1–4%, 1–2%), helium-hydrogen-methane (99–96%, 1–4%, 1–2%), and argon-nitrogen-methane (99–79%, 0–20%, 1%). Input 2.45 GHz microwave power was varied between 600–3000 W. Experimental field map curves such as those shown in Figs. 2 and 3 provided the operating substrate/pressure/power road map for this experimental investigation. At each operating pressure, optimum discharge uniformity, substrate temperature uniformity and hence deposition uniformity were achieved over the substrate diameter by careful adjustment of (1) microwave input power, (2) cavity tuning, and (3) stage height.

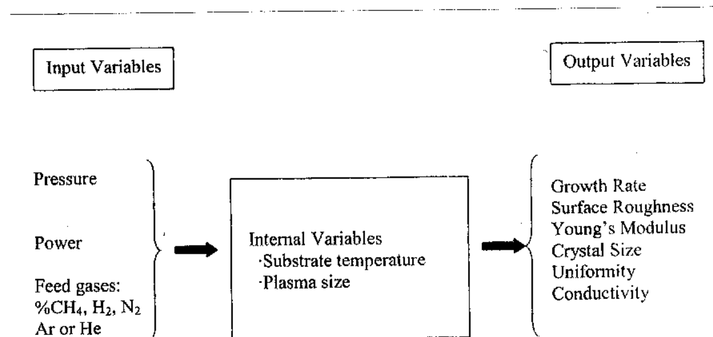

Fig. 4. Multivariate parameter space of microwave plasma-assisted diamond deposition.

The initial nucleation density of diamond on the substrate surface greatly influences the CVD synthesis of UNCD diamond films. Substrate pretreatment involved mechanical scratch seeding with 0.1 micron diamond powder followed by ultrasonic bath cleaning and acetone and deionized water rinse. The deposited films were characterized using high-resolution TEM to determine crystal size distribution, atomic force microscopy (AFM) to determine surface roughness, and SEM images of film cross section to determine film thickness and uniformity. The film thickness and consequently the measurement of the deposition rate was achieved by measuring the weight gain of the substrate after deposition. The Young's modulus of the film was measured using a laser acoustic technique based on creating a surface acoustic wave in the film and then determining the velocity of the propagating wave.[13] The electrical conductivity was measured using a four point probe measurement of the UNCD film grown on an insulating silicon dioxide layer.

4. Results and Discussion

The experimental results are organized into three groups: (1) argon-hydrogen-methane feed gas, (2) helium-hydrogen-methane feed gas and (3) argon-nitrogen-methane feed gas. For each of these groups, data showing growth rate and surface roughness are presented. For the selected feed gas groups, additional data on crystal size, film uniformity, Young's modulus and electrical conductivity are also presented.

4.1 *Argon-Hydrogen-Methane*

UNCD films can be successfully grown across a large input parameter space (60–180 Torr, 400–2000 W microwave power, hydrogen percentage 0–4% and methane 1–2%). Figure 5 shows growth rate versus methane flow rate. The growth rate increases up to 1.06

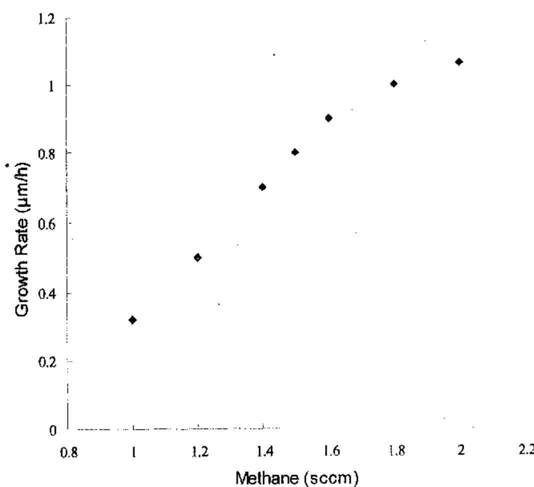

Fig. 5. Growth rate versus methane flow rate with $Ar:CH_4:H_2$ = 100: 1-2: 4 sccm and pressure=160 Torr.

μm/h at a methane flow rate of 2% and at a pressure of 160 Torr. Using 0–1% hydrogen, i.e., hydrogen deficient conditions, discharges were sustained in contact with the three inch substrates over a 60–200 Torr pressure regime. High-quality film deposition was extended to 240 Torr when H_2 concentrations were increased to 1–4%. Figure 6 shows growth rate versus pressure for three different hydrogen flow rates of 1, 2 and 4 sccm. The growth rate increases with pressure and, as observed in Fig. 2, the pressure has a strong influence on the substrate temperature. In fact, if the growth rate is plotted versus substrate temperature for different pressures and hydrogen flow percentages, growth rate monotonically increases with temperature as shown in Fig. 7. The fit of the data in Fig. 7 to an activation energy model is quite good and it gives a value of 25 kcal/mole. This value is close to that found for diamond growth with hydrogen-methane chemistry growth. The presence of this activation energy for hydrogen percentages of 1–4% in the input gas flow is consistent with the hydrogen abstraction reaction from the diamond growth surface being the dominant diamond growth rate control process. The influence of the hydrogen percentage on the substrate temperature is also a factor in the data presented in Fig. 6. If the other input parameters are held constant and the hydrogen percentage is increased from 1 to 2 to 4%, the substrate temperature typically increases by 10–25°C for each increment from 1 to 2% and then from 2 to 4%.

Further examination of the growth rate data shows an additional trend. Specifically, if the substrate temperature is held constant while the pressure is increased, for example by decreasing the hydrogen flow percentage as the pressure is increased, the growth rate increases. This phenomenon can be explained by an increase in the flux of growth species to the surface as the pressure increases resulting in an increase in growth rate even with the substrate temperature held constant.

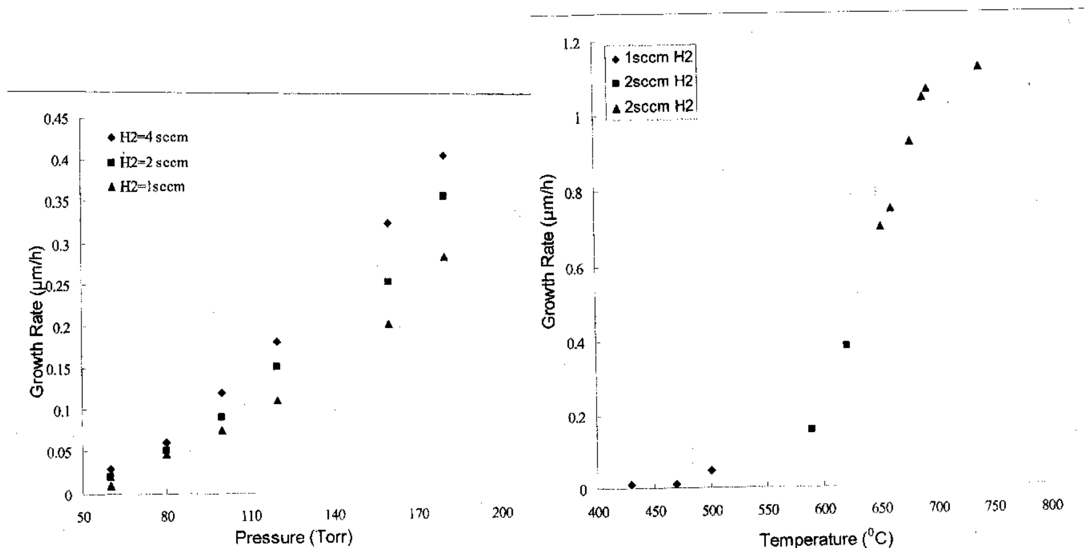

Fig. 6 (left). Growth rate versus pressure with $Ar:CH_4:H_2$ = 100:1:1-4 (sccm).
Fig. 7 (right). Growth rate versus substrate temperature with $Ar:CH_4:H_2$ = 100:1:1-4 sccm.

The influence of the hydrogen flow rate percentage from 1–4% on the growth rate is actually small if the influence of the hydrogen percentage variation on the substrate temperature is taken into account. An anomaly to this observation is when no hydrogen gas is added to the flow such that the input flow is just argon and methane. A specific example is when the substrate temperature is low (~400–500°C) and the hydrogen flow rate is 0% in the input gas flow, the growth rate is higher than that expected by the Arrhenius plot with an activation energy of 25 kcal/mole. For example, at 100 Torr with $Ar/H_2/CH_4$ at (99/2/1) and a microwave power of 1075 W, the substrate temperature is 490 and the growth rate is 0.089 μm/h. When the hydrogen is removed from the flow rate and the microwave power is set to 920 W with a pressure of 100 Torr, the substrate temperature decreases to 450 and the growth rate actually increases to 0.11 μm/h. This relatively high-growth rate at low temperatures when the hydrogen flow rate percentage is set to zero is consistent with the work of Xiao *et al.*[14] that showed growth rates of 0.2 μm/h at a pressure of 150 Torr and a substrate temperature of 400°C.

The surface roughness as measured by AFM scans for various input variables is shown in Fig. 8. The smoothest films are obtained with lower hydrogen flow percentages in the feed gas. The smoothest films have roughness values (rms) of 10–15 nm. The films do get rougher as they are grown to larger thicknesses as shown in Fig. 9. Films of one micron thickness show the smoothest values of 10–15 nm (rms). Thick films of 5–70 microns show roughness values of 30–65 nm rms.

The smoothness of the surface of the films deposited, particularly the smoothness of the very thick films of up to 70 μm thick, indicates that the film growth occurs by renucleation that produces small crystal sizes. A more accurate measure is the actual crystal size distribution. The crystal size distributions were measured using TEM dark-field imaging. For a UNCD film grown at 120 Torr with a gas mixture of argon-100 sccm, hydrogen-4 sccm and methane-1sccm, the distribution ranged from 3 to 12 nm as shown in Fig. 10.[10] The

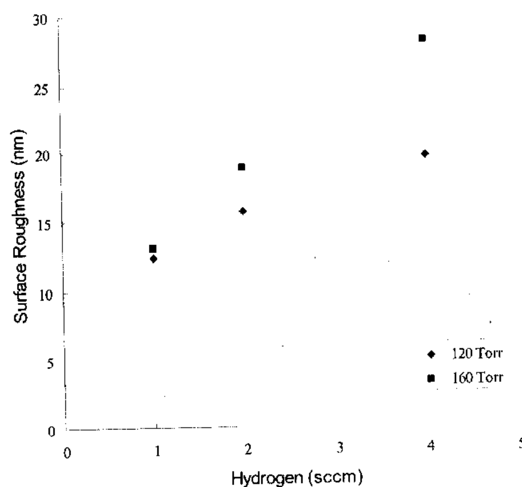

Fig. 8. Surface roughness versus hydrogen flow rate with $Ar:H_2:CH_4$ = 100:1-4:1 (sccm)

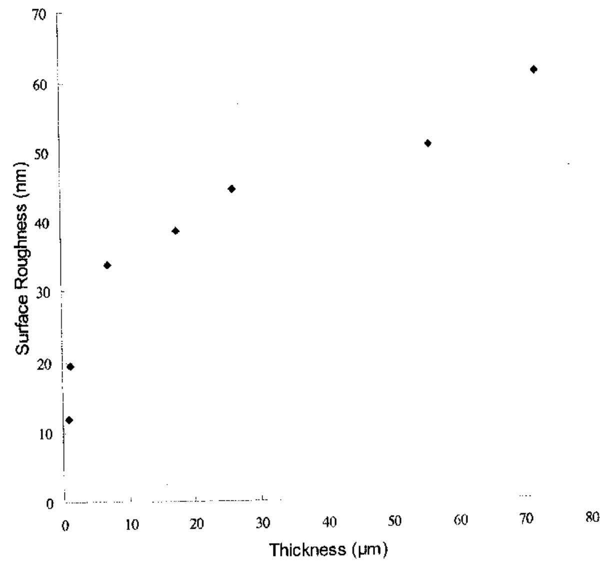

Fig. 9. Surface roughness versus film thickness with $Ar:H_2:CH_4$ = 100:4:1-2 (sccm).

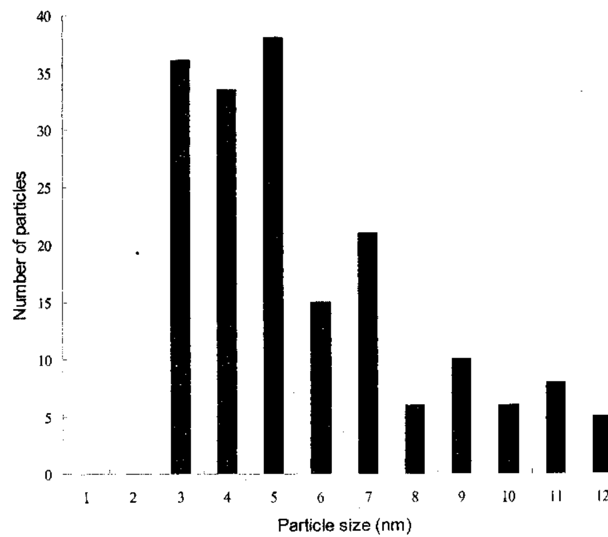

Fig. 10. Crystal size distribution of UNCD film determined by TEM dark-field imaging with 120 Torr, $Ar/H_2/CH_4$ =100/4/1 sccm, and deposition time = 8 h.

predominant crystal sizes in the distribution were 3–7 nm. Note that the sample selected had a 4% hydrogen flow rate in the gas flow. It is expected that the crystal size distribution will have even more smaller crystal sizes for the lower hydrogen concentrations.

The Young's modulus of selected films has also been measured to assess the mechanical properties of the films. Young's modulus data was reported by Reinhard *et al.*[13] for three ultrananocrystalline films all grown at 120 Torr with 100/1/1 ($Ar/H_2/CH_4$). The Young's moduli measured were 840–930 GPa. For comparison, values reported for previous UNCD results include an average of 886 GPa measured using nanoindentation,[15] a range of 916–959 GPa measured using microcantilever deflection,[16] and a range of 930–970 measured using microscale membrane deflection.[16]

One important consideration for the deposition of UNCD for applications is the uniformity of the deposition across the 7.5-cm-diameter substrates that were used in this study. Figure 11 shows the uniformity deposition across the 7.5 cm-diameter substrate versus pressure and feed gas composition. Uniformity is defined as the thinnest region divided by the thickest region.

4.2 *Helium-Hydrogen-Methane*

As an alternative to argon as the inert gas, the use of helium was investigated. Figure 12 and 13 show the growth rates and surface roughness. Similar to the argon inert gas case, the growth rate increases with increasing hydrogen percentage in the feed gas. As the hydrogen percentage increases from 1 to 4%, the substrate temperature increases from 630 to 685°C for the data in Fig. 12. As indicated in Fig. 13, using He as the inert gas, the surface roughness value behavior versus H_2 gas is very similar to the argon gas case. The thicknesses of the films shown for the 1, 2, and 4% H_2 were 0.6, 0.84 and 1.8 μm, respectively.

4.3 *Argon-Nitrogen-Methane*

The addition of nitrogen gas to the feed gas in place of hydrogen has a similar effect on growth rate and surface roughness as shown in Figs. 14 and 15. The nitrogen addition increases growth rate and surface roughness. The addition of nitrogen also makes the films

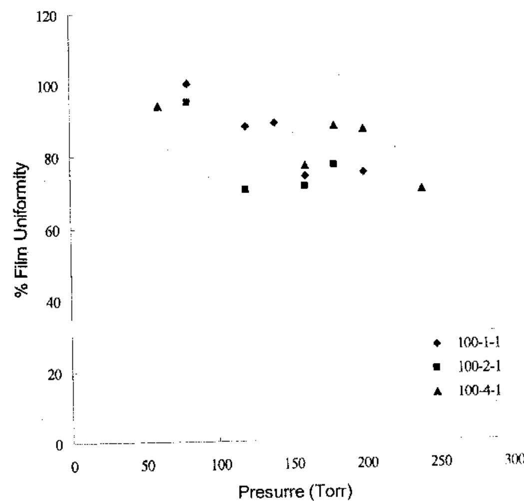

Fig. 11. Percent uniformity across 7.5-cm-diameter substrate versus pressure with $Ar-H_2-CH_4$ indicated in legend.

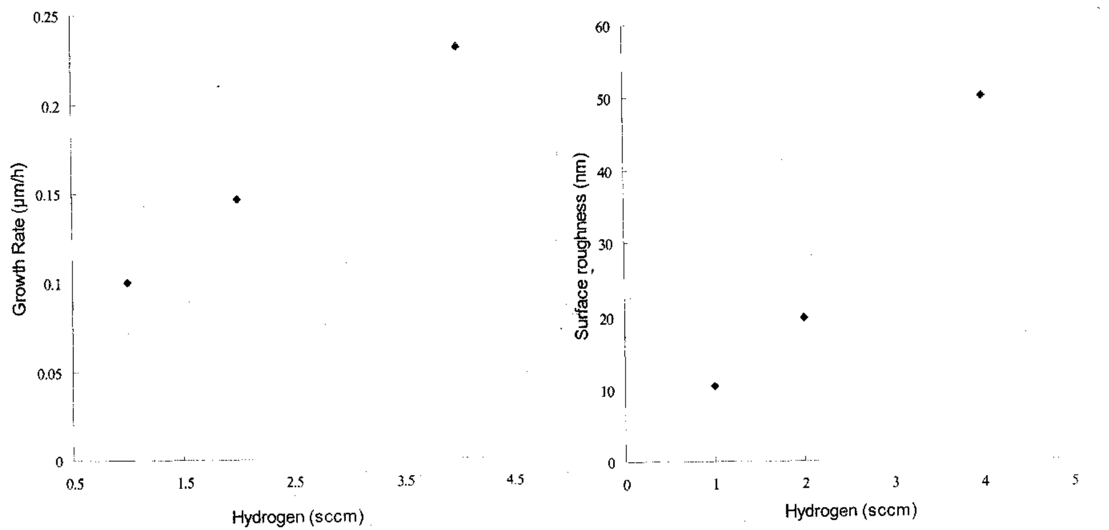

Fig. 12 (left). Film growth rate versus hydrogen flow rate with pressure =120 Torr and gas mixture of He:CH_4:H_2 = 100:1:1-4 sccm.
Fig. 13 (right). Film surface roughness versus hydrogen flow rate with pressure =120 Torr, gas mixtures He:CH_4:H_2 = 100:1:1-4 sccm, and deposition time = 8 h.

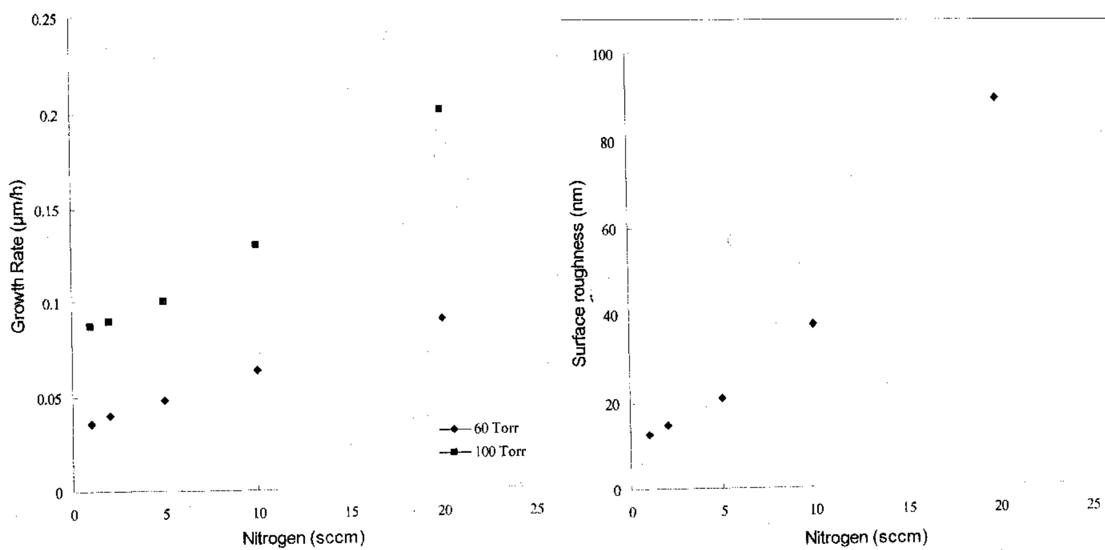

Fig. 14 (left). Film growth rate versus nitrogen flow rate with Ar:CH_4:N_2 = 100:1:1-20 sccm.
Fig. 15 (right). Surface roughness versus nitrogen flow rate with pressure 100 Torr and Ar:CH_4:N_2 = 100:1:1-20 sccm.

electrically conducting. The conductivity of the films as measured using a four point probe is shown in Fig. 16. The conductivity increases as the nitrogen percentage in the feed gas is increased.

5. Summary

Using argon-hydrogen-methane and helium-hydrogen-methane input gas mixtures and a thermally floating substrate, uniform, low-stress UNCD films have been deposited over a wide pressure range (60–180 Torr) and temperature range (400–800°C). Films were grown on 3-inch-diameter silicon substrates with a thickness ranging from 58 nm to >50 μm. A film surface roughness as low as 10 nm was obtained by AFM. Film roughness increased as pressure and hydrogen percentage in the gas mixture increased. The growth rate increased as pressure, gas mixture (%H_2, %CH_4), and microwave power increased. A high growth rate of 1.12 μm/h was achieved at 180 Torr, $H_2/Ar/CH_4$ = (4:100:2) sccm and 1.5 kW absorbed power. Optimized film uniformities of 75–95% were achieved with average growth rates of more than 0.5 μm/h. If lower growth rates are acceptable, then uniformities that approach 100% are achievable. Overall, a robust, repeatable process has been demonstrated for the deposition of UNCD films. It appears that these process techniques and methodologies can readily be scaled to larger 10-cm-diameter wafers in the current 2.45 GHz microwave plasma reactor system. Using the same experimental methodology, this UNCD synthesis process can be developed and scaled to even larger 15–20-cm-diameter areas by directly scaling up the microwave reactor technology so that it operates with 915 MHz excitation. Deposition rates and uniformity may also be improved by adding heater technologies to the existing reactor system.

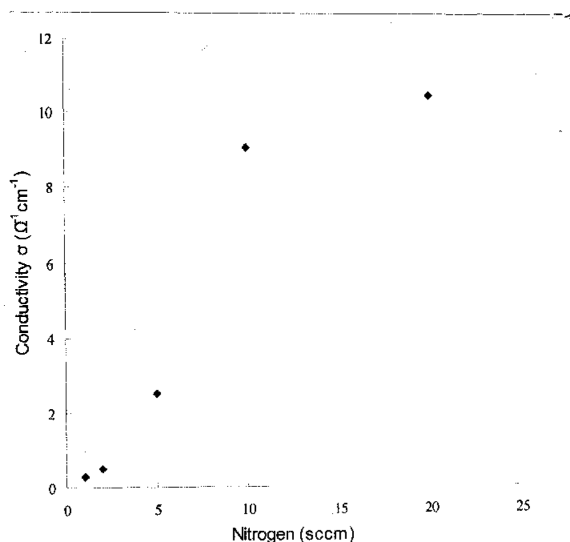

Fig. 16. Room temperature conductivity versus nitrogen flow rate with pressure=100 (Torr) and $Ar:CH_4:N_2$ = 100:1:1-20 sccm.

Acknowledgement

The authors acknowledge the National Science Foundation for support under MRSEC program grant DMR-9809688 and also support from the Fraunhofer USA Center for Coatings and Laser Applications.

References

1) D. Zhou, D. M. Gruen, L. C. Qin, T. G. McCauley and A. R. Krauss: J. Appl. Phys. **84** (1998) 1981.
2) H. D. Espinosa, B. Peng, B. C. Prorok, N. Moldovan, O. Auciello, J. A. Carlisle, D. M. Gruen and D. C. Mancini: J. Appl. Phys. **94** (2003) 6076.
3) A. Erdemir, G. R. Fenske, A. R. Krauss, D. M. Gruen, T. McCauley and R. T. Csencsits: Surf. Coat. Technol. **120–121** (1999) 565.
4) S. Bhattacharyya, O. Auciello, J. Birrell, J. A. Carlisle, L. A. Curtiss, A. N. Goyette, D. M. Gruen, A. R. Krauss, J. Schlueter, A. Sumant and P. Zapol: Appl. Phys. Lett. **79** (2001) 1441.
5) M. Hupert, A. Muck, R. Wang, J. Stotter, Z. Cvackova, S. Haymond, Y. Show and G. M. Swain: Diamond Relat. Mater. **12** (2003) 1940.
6) A. Krauss, O. Auciello, D. Gruen, A. Jayatissa, A. Sumant, J. Tucek, D. Mancini, M. Molodvan, A. Erdemir, D. Ersoy, M. Gardos, H. Busmann, E. Meyer and M. Ding: Diamond Relat. Mater. **10** (2001) 1952.
7) B. Bi, W. S. Huang, J. Asmussen and B. Golding: Diamond Relat. Mater. **11** (2002) 677.
8) W. Yang, O. Auciello, J. E. Butler, W. Cai, J. A. Carlisle, J. E. Gerbi, D. M. Gruen, T. Knickerbocker, T. L. Lasseter, J. N. Russell, L. M. Smith and R. J. Hamers: Nature Mat. **1** (2002) 253.
9) K. P. Kuo and J. Asmussen: Diamond Relat. Mater. **6** (1997) 1097.
10) Wen-Shin Huang, PhD Dissertation, Michigan State University, 2004.
11) T. A. Grotjohn and J. Asmussen: Ch 7 in *Diamond Films Handbook* Ed. J. Asmussen and D. K. Reinhard (Marcel Dekker, New York, 2002) p. 211-302, particularly 217-219.
12) W. S. Huang, D. T. Tran, J. Asmussen, T. A. Grotjohn and D. K. Reinhard: Diamond Relat. Mater. (in press).
13) D. K. Reinhard, T. A. Grotjohn, M. Becker, M.K. Yaran, T. Schuelke and J. Asmussen: J. Vac. Sci. and Technol. B **22** (2004) 2811.
14) X. Xiao, J. Birrell, J. E. Gerbi, O. Auciello and J. A. Carlisle: J. Appl. Phys. **96** (2004) 2232.
15) A. V. Sumant, O. Auciello, A. R. Krauss, D. M. Bruen, D. Ersoyh, J. Tucek, A. Jayatissa, E. Stach, N. Moldovan, D. Mancini, H. G. Busmann and E. M. Meyer: Mater. Res. Soc. Symp. Proc. **657** (2000) EE5.33.
16) B. C. Prorok, H. D. Espinosa, J. E. Butler, S. Chattopadhyay, K. H. Chen and L. C. Chen: J. Appl. Phys. **93** (2003) 2164.